Published in final edited form as:
J Phys Chem B. 2009 April 2; 113(13): 4248–4256. doi:10.1021/jp810685g.

UV Resonance Raman Determination of Molecular Mechanism of Poly(N-Isopropylacrylamide) Volume Phase Transition

Zeeshan Ahmed, **Edward A. Gooding**, **Konstantin V. Pimenov**, **Luling Wang**, and **Sanford A. Asher**
Department of Chemistry, University of Pittsburgh, PA 15260, Phone: 412 624 8570, Fax: 412 624 0580, Email: asher@pitt.edu

Abstract

Poly (*N*-isopropylacrylamide) (PNIPAM) is the premier example of a macromolecule that undergoes a hydrophobic collapse when heated above its lower critical solution temperature (LCST). Here we utilize, dynamic light scattering, H-NMR, steady-state and time-resolved UVRR measurements to determine the molecular mechanism of PNIPAM's hydrophobic collapse. Our steady-state results indicate that in the collapsed state the amide bonds of PNIPAM do not engage in inter-amide hydrogen bonding, but are hydrogen bonded to water molecules. At low temperatures, the amide bonds of PNIPAM are predominantly fully water hydrogen bonded, whereas, in the collapsed state one of the two normal C=O hydrogen bonds is lost. The NH-water hydrogen bonding, however, remains unperturbed by the PNIPAM collapse. Our kinetic results indicate a mono-exponential collapse with τ~360 (±85) ns. The collapse rate indicates a persistence length of n~10. At lengths shorter than the persistence length the polymer acts as an elastic rod, whereas, at lengths longer than the persistence length the polymer backbone conformation forms a random coil. Based on these results we propose that at low temperatures PNIPAM adopts an extended, water-exposed conformation that is stabilized by favorable NIPAM-water solvation shell interactions which stabilize large clusters of water molecules. At elevated temperatures, thermal agitation disrupts these interactions. The PNIPAM+water polymer undergoes a volume phase transition, expels water and shrinks to a compact conformation that reduces its hydrophobic solvent accessible surface area. In this compact state, PNIPAM forms small hydrophobic nano-pockets where the (*i*, *i* +3) isopropyl groups make hydrophobic contacts. A persistent length of n~10 suggests a cooperative collapse where hydrophobic interactions between adjacent hydrophobic pockets stabilize the collapsed PNIPAM.

Keywords

Hydrophobic Collapse; NIPAM; volume phase transition; Raman; cold denaturation; dehydration; amide; chemo-mechanical; sensors

INTRODUCTION

Poly(*N*-isopropylacrylamide) (PNIPAM) is the premier example of a macromolecule that undergoes a hydrophobic collapse when heated above its lower critical solution temperature (LCST).[1–17] Below its LCST, PNIPAM exists in a swollen, well-hydrated state that is nearly refractive index matched to water; the polymer weakly scatters light.[1–6,18,19] At the transition temperature (T_t~32–35 °C) the polymer undergoes a hydrophobic collapse, expels water and adopts a compact state[3,5,6] and shows a dramatic increase in turbidity.

Correspondence to: Sanford A. Asher.

This temperature dependent PNIPAM collapse, which in the physics community is called a "volume phase transition" (VPT) [1–6,19] gives rise to very large volume changes for cross-linked PNIPAM, which can be used to actuate chemical and physical phenomena. This VPT has been utilized in drug delivery,[20,21] synthesis[22,23] (where PNIPAM serves as a nanoreactor) and sensor development.[3,24,25] For these applications, PNIPAM nanogels are functionalized such that environmental changes induce PNIPAM chemical changes (e.g. deprotonation of a carboxylic acids) that shift the PNIPAM's critical transition temperature. The PNIPAM hydrophobic collapse can thus be designed to occur in response to a specific chemical stimulus such as pH changes.[26–29]

The PNIPAM hydrophobic collapse results from the temperature dependence of PNIPAM-water interactions.[27,28,30–33] Presumably, at low temperatures the favorable enthalpy of amide-water hydrogen bonding stabilizes the swollen state of PNIPAM by overcoming the unfavorable entropy of water solvation of the isopropyl hydrophobic groups.[34] As the temperature increases towards the VPT the unfavorable hydrophobic solvation entropy eventually dominates, forcing the PNIPAM collapse, releasing water into the bulk. Recent dielectric relaxation studies suggest that the average number of hydrating water molecules per NIPAM group falls from 11 to ~ 2 upon the hydrophobic collapse.[35,36]

The temperature dependence of the entropy-enthalpy balance determines the critical VPT temperature. This VPT is similar to the "inverse temperature transition" of elastin-like peptides that undergo well-known transitions from an extended, highly mobile conformation to a collapsed molten globule-like conformation at higher temperatures.[37–41] This VPT of PNIPAM and elastin-like peptides is related to the cold-denaturation[42–48] phenomenon observed in proteins such as myoglobin. Proteins typically undergo a transition from a native compact state to disordered, expanded state as the solution temperature *decreases*.[49,50] Protein cold denaturation appears also to be driven by the temperature dependence of the free energy of solvation of the hydrophobic groups.[50] At higher physiological temperatures, the low hydrophobic solvation entropy favors compact or folded protein conformations where hydrophobic groups are protected from water. At lower temperatures expanded conformations with hydrophobic groups exposed to water become stabilized over the folded, compact conformations.[42–50]

There is intense interest in developing a molecular understanding of the molecular mechanism of PNIPAM's VPT. In the work here, we probe this VPT using monodisperse, highly charged PNIPAM nanogels which undergo the VPT.[3,51] This simple homogeneous system can be straight-forwardly studied and the VPT here is not confounded by processes such as polymer aggregation.

Kinetic studies of macroscopic PNIPAM hydrogels find that the rate of polymer collapse should scale as l^{-2}, where l is the smallest dimension of the material.[52,53] Thus, PNIPAM nanogels are expected to show relatively fast collapse kinetics, as compared to macroscopic gels that take hours or days.[3] Indeed, Wang *et al*'s[1] T-jump kinetic turbidity measurements of ~400 nm diameter PNIPAM nanoparticles showed a single exponential collapse with an apparent time constant of ~390 ns. In addition, Reese *et al*[3] utilized kinetic turbidity measurements following a laser induced T-jump to examine the collapse of ~350 nm diameter PNIPAM nanogels and observed a multi-exponential process with a major component occurring in less than 1 μs.[3] Reese *et al*[3] also showed that individual PNIPAM nanoparticles show an apparent single exponential collapse with $\tau \sim 120$ ns.

To date most spectroscopic studies of the PNIPAM's hydrophobic collapse have focused on its steady state behavior. Utilizing FTIR,[34,54–59] ATR/FTIR[60] and Raman spectroscopy[27,28,30,31,33] several groups independently determined that PNIPAM's hydrophobic collapse

disrupts the hydration of both hydrophobic and hydrophilic groups. In particular, FTIR[34, 54–59] and ATR/IR[60] studies focusing on the AmI region (C=O stretch) showed that hydrogen bonding of the amide carbonyl changes with temperature. The consensus appears to be that the hydrogen bonds present at low temperatures are disrupted upon the higher temperature PNIPAM hydrophobic collapse.

In this study we utilize steady-state and time-resolved UV resonance Raman (UVRR) spectroscopy to directly examine the equilibrium and kinetics of amide dehydration during the PNIPAM's hydrophobic collapse. Our results indicate that the amide dehydration is complete within ~1 μs.

Experimental

The ~170 nm diameter PNIPAM nanoparticles (T_t ~33 °C) were synthesized using previously published techniques.[51] Briefly, the PNIPAM particles were synthesized by dispersion polymerization. 1.40 g NIPAM (Aldrich, used after recrystallization), 0.0242 g 2-acrylamido-2-methyl-1-propanesulfonic acid (ionic co-monomer, Aldrich), 0.0659 g N, N′-methylenebisacrylamide (cross-linker, Fluka), 0.036 g sodium dodecyl sulfate (surfactant, Aldrich) and 0.088 g ammonium persulfate (initiator, Sigma-Aldrich) were added to 100 mL 18 MΩ deionied water and reacted at 70 °C for 4 hr under stirring. The crude product was filtered by glass wool and dialysized against DI water by using a Snakeskin™ dialysis tube (10,000 MWCO) for 2 weeks to remove impurities such as unreacted NIPAM monomers, dodecyl sulfate and single chains. Deuterium labeled d_7-PNIPAM monomers (the isopropyl group hydrogens are deuterated) were acquired from Cambridge Isotopes and used to synthesize ~100 nm diameter d_7-PNIPAM particles. Temperature dependent changes in particle size were measured by dynamic light scattering (ZetaPALS, Brookhaven Instruments Corporation).

The solid sample of dried PNIPAM nanoparticles was prepared by allowing a sample of PNIPAM particles to slowly dehydrate at room temperature under a steady flow of dry nitrogen gas.

The hydrogen-deuterium exchange (HDX) studies were carried out on a 300 MHz high-field H-NMR instrument (Bruker). A 100 μl solution of 0.73% wt/vol of PNIPAM in water at 20° and 55 °C was diluted with D_2O (at 20° and 55 °C, respectively) to a final volume of 1 mL. All H-NMR spectra were immediately acquired following solution preparation at 20° and 55 °C, except for one room temperature H-NMR spectra which was allowed to sit for 24 hr to rule-out any slow exchange. The time between solution preparation and spectral acquisition was less then 5 min. The 20 °C NMR spectra of PNIPAM in H_2O only was acquired utilizing 850 μl of stock PNIPAM solution with 50 μl of CD_3CN for deuterium locking.

A home built UV resonance Raman (UVRR) spectrometer was used for both steady-state and kinetic measurements.[61] The T-jump results were obtained with a home-built nanosecond pump-probe setup. The probe laser was a 1 kHz repetition rate Photonics Industries Ti:Sapphire laser which produced ~204-nm laser light with an average energy of 2.4 μJ per pulse and a pulsewidth (FWHM) of 14 ns. The output beam was collimated and focused to a spot size of ~ 100 μm at the sample.

The pump laser was a 1 kHz repetition rate Photonics Industries YLF-pumped OPO, which produced 1.9 μm pulses with an average energy of 1 mJ per pulse and a pulse width of 13 ns. The IR beam was collimated, made collinear with the UV beam and focused to a spot size of ~165 μm at the sample. The pump and probe lasers were synchronized and a variable delay was obtained by using a digital pulse generator (DG535, Stanford Research systems, Inc).

These delay times were confirmed by measuring reflections of the pump and probe pulses with fast photodiodes by using an oscilloscope (TDS 3054B, Tektronix).

A 10 mL solution of 0.73% wt/vol PNIPAM nanoparticles was circulated in a free surface, temperature controlled stream. The concentration of PNIPAM was chosen to match the sample absorption for both the UV probe ($OD_{204\,nm}$ = 156) and IR pump laser. This ensures that during the T-jump experiment, the UV laser probes the heated volume of the sample stream.[62]

A ~165° laser excitation backscattering geometry was used for sampling. The collected light was dispersed by a subtractive double monochromator onto a back thinned CCD camera (400 B Princeton Instruments-Spec 10 System).[61] Four 2 min. spectra were averaged.

The magnitude of the T-jump was determined from the UVRR water O-H stretching region which is highly temperature dependent.[62,63] T-jump spectra were compared to equilibrium spectra taken at different temperatures (data not shown), demonstrating a ~15 °C T-jump from the initial equilibrium temperature of 30 °C to a final temperature of 45 °C.

The steady-state UVRR spectra were acquired on the same spectrometer by using only the probe laser. The UVRR PNIPAM spectra in the amide region taken with and without T-jumps were normalized to the intensity of the isopropyl group's CH_3 deformation band at ~1460 cm^{-1} and subtracted from the equilibrium 30 °C spectrum.

The transient difference feature in the AmI region was fitted to the convolution of a Gaussian instrument function with the sum of a step function and an exponential rise. The step function accounts for the essentially instantaneous spectral changes due to the T-jump which were not associated with PNIPAM structural changes, while the exponential rise time derives from the dynamics of the polymer structural collapse. The 22 ns width of the Gaussian instrument function is due to the pump and probe laser pulse widths and the 15 ns timing jitter. The instrument function was determined by fitting the difference Raman signal in the water O-H stretching region around 3300 cm^{-1}. The T-jump gives rise to an essentially instantaneous temperature change, since thermalization of near-IR laser excitation in water is known to occur on the psec timescale.[63]

Results and Discussion

DLS measurements

The Fig 1 temperature dependent DLS measurements indicate that between 4 °C and 45 °C the particle size collapses from 167 nm to 80 nm, with a transition temperature T_t ~ 33 °C. The PNIPAM particles undergo a hydrophobic collapse from a high-volume water-swollen state to a 9-fold smaller volume, compact state.[3,5,6] The volume change suggests an ~88% reduction in water molecules inside the PNIPAM particles, which represents a loss of ~$8.7*10^7$ water molecules for the ~$2.4*10^6$ amide bonds in the nanogels particle a ratio similar to the 81% loss in water hydration estimated by Ono *et al*.[36]

UVRR spectral band assignments

The 204-nm excited UVRR spectra of PNIPAM (Fig 2) resemble the typical amide spectra seen for proteins. We observe a broad AmI band (predominantly C=Os)[64–66] at 1625 cm^{-1} while, the AmII band (predominantly C-N_s with NH_b)[66,67] is located at 1565 cm^{-1}. The resonance enhanced $C_\alpha H_b$ band[68–70] is located at 1387 cm^{-1}. Two weak AmIII bands are observed at 1345 and 1321 cm^{-1}, whereas, a strong AmIII band (C-N_s with NH_b)[66,67] located at 1258 cm^{-1} shows shoulders at 1284 cm^{-1} and ~1230 cm^{-1}. It should be noted that a similar molecule, *N*-methylacetamide shows only a single intense AmIII band at 1315 cm^{-1}.[66,67,

[71] Likely, the multiple AmIII bands in PNIPAM arise due to coupling between the AmIII vibration (C-N_s with NH_b) and isopropyl group vibrations.

In order to ascertain the impact of the pendent isopropyl group on amide vibrations we examined the 204-nm excited UVRR spectra of deuterium labeled d_7-PNIPAM. In d_7-PNIPAM the seven hydrogen atoms of the isopropyl group have been replaced with deuterium atoms (Fig 3). The largest impact of deuterium labeling is observed in the AmII region (Fig 2) where deuterium labeling broadens and downshifts the AmII band ((ΔFWHM = 2 cm-1, Δν = 7 cm^{-1}). This result indicates that the normal mode composition of the AmII vibration in PNIPAM contains significant contribution from the isopropyl group motion.

Upon deuteration, the weak ~1460 cm^{-1} band of PNIPAM is replaced by a broad low intensity feature centered around ~1445 cm^{-1} (d_7-PNIPAM, Fig 2). The 1460 cm^{-1} band of PNIPAM derives from a non-resonant enhanced CH_3 deformation mode of the isopropyl group.[72]

Deuterium labeling decreases the 1387 cm^{-1} $C_\alpha H_b$ band intensity but does not significantly impact the band frequency. The 1387 cm^{-1} band in the natural abundance NIPAM has a ~50% contribution from isopropyl CH_3 umbrella motion. The d_7-PNIPAM completely derives from the amide $C_\alpha H$ bending vibration (Fig 3).

In the AmIII region deuterium labeling appears to only impact the AmIII bands at 1300 cm^{-1}, 1345 cm^{-1} and 1321 cm^{-1}. The frequencies of the strong AmIII band centered at 1258 cm^{-1} and its shoulders at ~1284 cm^{-1} and 1230 cm^{-1} are not impacted by isopropyl group deuteration (Fig 2). Upon deuteration both the 1345 cm^{-1} and 1321 cm^{-1} AmIII bands of PNIPAM appear to have been replaced by a single band located at ~1341 cm^{-1} (Fig 2). The difference spectrum between d_7-PNIPAM and PNIPAM shows a positive peak at ~1300 cm^{-1}.

This result indicates that both the 1345 cm^{-1} and 1321 cm^{-1} and 1300 cm^{-1} AmIII bands contain significant contribution from isopropyl vibrations. We, therefore, conclude that the 1345 cm^{-1} and 1321 cm^{-1} AmIII bands of PNIPAM are not the same vibrations as the $AmIII_1$ and $AmIII_2$ vibrations observed in peptides which derive from coupling between the AmIII vibration and the heavy atom vibrations of the peptide backbone.[67]

As noted above the frequencies of the AmIII bands located in the region of 1200-~1290 cm^{-1} are not impacted by deuterium labeling of PNIPAM's isopropyl group (Fig 2). This result indicates that the AmIII bands located in this region do not contain a significant contribution from the isopropyl group and, thus, derive from the "classical AmIII" vibration[67] which is predominantly C-N_s stretching coupled with in-phase NH_b motion.[66,67] Extensive Raman studies indicate that the "classical" AmIII vibration is sensitive to hydrogen bonding and dihedral angle changes around the C_α-C bond length (see Fig 3).[67,69,73] In peptides this vibration is referred to as the $AmIII_3$ vibration.[67] In subsequent discussion, we refer to this band as simply the AmIII band.

Temperature dependence of PNIPAM

As the temperature is increased from 4 to 65 °C the AmI band of PNIPAM shows a ~28 cm^{-1} upshift from 1623 to 1651 cm^{-1} and its intensity increases by ~15% (Fig 4) suggesting a T_t ~ 37 °C. We can model the spectral changes in the AmI region by using three Gaussian bands located at 1624 cm^{-1}, 1655 cm^{-1} and 1700 cm^{-1} (Fig 5). The low intensity 1700 cm^{-1} AmI feature likely derives from dehydrated amides, while the 1624 cm^{-1} band derives from fully hydrogen bonded amides at least 2 waters hydrogen bonded at the C=O (hydrogen bonded at sites A and C, Fig 5A) and one water hydrogen bonded at the N-H site (hydrogen bonded at the B site).[74,75] The 1655 cm^{-1} AmI band, which occurs ~30 cm^{-1} to higher frequency from

the fully hydrogen bonded AmI band, probably derives from an intermediate hydrogen bonded state, with only two hydrogen bonded waters, one each at the C=O and N-H sites[74,75] (hydrogen bonded at the A and B sites).

The AmI spectral changes result from changes in the intensity ratio of the 1624 cm^{-1} and 1654 cm^{-1} AmI bands over the 30–40 °C temperature range (Fig 6). Obviously, the PNIPAM's hydrophobic collapse decreases the hydration of the pendent amide bonds increasing the intensity of the higher frequency 1654 cm^{-1} AmI band. At low temperature the 1624 cm^{-1} band dominates indicating that most of the amide bonds are fully hydrogen bonded at all three sites (A, B, and C), while above 30 °C the amides predominantly show A and B hydrogen bonding. Our spectral modeling suggests (assuming similar Raman cross sections) that the PNIPAM collapse results in a hydration change, where at low temperature fully hydrated amides, which constitute ~60 % of the population decreases to ~40 % of the population at the higher temperature. The less hydrated A and B site hydrogen bonded amide population increases from ~ 30 % to 50 % of the population. The fully dehydrated amide population decreases only slightly. The presence of multiple AmI bands-representing various degrees of amide hydrogen bonding even at low temperatures, indicates that pockets of collapsed polymer, hydrophobic domains are present at all temperatures.

The intensity ratio of the (1655/1624) cm^{-1} AmI bands does not show any significant change until the solution temperature increases above 30 °C. Light scattering (Fig 1), in contrast, shows a ~24% decrease in particle diameter (and a 56% volume decrease) between 15 °C and 30 °C. This indicates that a large particle volume decrease occurs due to the temperature increase to 30 °C in the absence of any obvious Raman changes in the amide hydration level.

Previously, Manas *et al*[76] utilizing IR spectroscopy demonstrated that burial of an amide bond inside protein's hydrophobic core upshifts the AmI band by ~26 cm^{-1} as compared to a water-exposed amide.[76] This upshift in the AmI band frequency derives from a weakening/loss of hydrogen bonding[64,76–78] and a decrease in the dielectric constant of the surrounding media.[78,79] Theoretical studies suggest that the dielectric constant in the protein's hydrophobic interior is ε ~ 4–20.[80–82]

Recently, Iwai *et al*[25] utilized a florescent dye, 9,-(4-N, N-dimethylaminophenyl) phenanthrene to probe the local dielectric constant in a PNIPAM hydrogel. These authors interpreted the temperature induced shift in λ_{max} of the fluorescence as arising due to a change in the dielectric constant of the surrounding media. They suggest that at 40 °C (above the LCST) the local dielectric constant in the collapsed state of PNIPAM is ~17, while at 15 °C the local dielectric constant is ~ 63, close to that of pure water.[25] The relatively high dielectric constant of the high temperature PNIPAM nanoparticles indicates significant water penetration of the collapsed particle's interior.

Recently, Ono *et al*[36] utilized dielectric relaxation methods to estimate that in the collapsed state of PNIPAM the number of hydrating water molecules is ≤ 2 per NIPAM group. In contrast, the low temperature hydrated state boasts ~11 water molecules per amide group.[36]

The loss/weakening of amide hydrogen bonding observed in the AmI region is confirmed by spectral changes in the AmII and AmIII region. The AmII band systematically loses 10% of its intensity while the AmI band intensity shows a ~15% increase as the temperature increases from 4 to 65 °C. Previously, Triggs and Valentini[83] observed that upon water hydrogen bonding, the AmI band intensity of *N*-methylacetamide (NMA), a model amide bond, decreases while the AmII band intensity increases. The ratio of the AmI to AmII intensity also increases as the solvent polarity increases.[70,83,84] These authors suggest that hydrogen bonding stabilizes the charged resonance form of the amide bond [$^{-}O(C)=NH^{+}$]. This makes the ground state geometry more like that of the excited state along the C=O coordinate and less like that

of the excited state along the C-N coordinate, thus diminishing the displacement along the C=O bond and increasing the displacement along the C-N bond. Consequently, hydrogen bonding results in a relatively smaller resonance enhancement of the AmI vibration and a greater enhancement of the AmII vibration.[83]

The AmII and AmIII band frequencies downshift with increasing temperature. The AmII band downshifts from 1565 to 1558 cm^{-1} while the AmIII band downshifts from 1258 to 1252 cm^{-1} as the temperature increases from 4 to 65 °C (Fig 4). Similar temperature-dependent changes in the AmII and AmIII frequencies have been observed for water-exposed peptide bonds[67,85,86] and attributed to temperature induced weakening and/or loss of amide-water hydrogen bonding.[62,67,76]

It should be noted that changes in AmII and AmIII frequencies are ~5 times smaller then the upshift in the AmI frequency. This result is highly unusual. Typically, the temperature induced frequency shifts are largest for the AmII vibration (−0.11 cm^{-1}/°C), followed by the AmIII vibration (−0.09 cm^{-1}/°C) with the AmI vibration showing a smaller upshift.[67]

Utilizing high level density functional theory calculations of NMA and NMA-water complexes we recently demonstrated that the AmI vibration is predominantly sensitive to changes in hydrogen bonding at the C=O, while the AmII vibration is almost exclusively sensitive to hydrogen bonding at the N-H site.

Assuming the amide vibrations in PNIPAM and NMA have similar normal mode compositions we can conclude that the AmI frequency shift indicates an increase in the A (C=O) and B (N-H) site water hydrogen bonded amide population. A lack of significant change in the AmII frequency indicates little or no change in hydrogen bonding at the B site. The results drawn from both the AmI and AmII frequency shifts indicate little or no change in N-H hydrogen bonding, while a decrease in hydrogen bonding occurs at the C=O.

We also examined the exposure of the amide groups by measuring their hydrogen-deuterium exchange rates at room temperature and 55 °C. We found that all the amide N-H were exchanged within the ~5 min it took to prepare and measure the H-NMR spectra (data not shown). This result clearly indicates that the collapsed PNIPAM does not significantly hinder diffusion of D_2O into the collapsed particle. This result, thus, indicates that in the collapsed state of PNIPAM, the amide bonds are hydrogen bonded to water and not to each other.

The 1387 cm^{-1} $C_\alpha H_b$ bending band shows no significant temperature-induced frequency or intensity change. Previous studies indicate that the $C_\alpha H_b$ band intensity is greatest when the $C_\alpha H$ and amide N-H bonds are *cis*, which allows for maximum coupling.[69,87] However, in the *trans* conformation the two bonds lie far from each other giving minimal coupling. In proteins, the *cis* C_α-H bond conformation corresponds to an extended β-strand while the *trans* conformation corresponds to α-helix-like conformation.[69] The lack of change in the $C_\alpha H_b$ band during PNIPAM's hydrophobic collapse thus indicates essentially identical Ramachandran Ψ angles for the collapsed and fully hydrated PNIPAM conformations. Further, the AmII and AmIII features at both low and high temperatures demonstrate that the amide bond conformation remains in the trans amide form throughout the VPT.

We compared the collapsed form of PNIPAM in water to that of fully dried PNIPAM prepared by flowing dry nitrogen over the sample. As compared to the collapsed particles in water (45 °C), the dry, solid PNIPAM at room temperature AmI band intensity is dramatically increased and its frequency is upshifted by 7 cm^{-1}, while its band width (ΔFWHM = 5 cm-1) significantly narrows (Fig 7). The solid PNIPAM AmII vibration shows a 7 cm^{-1} downshift in the dry, solid state whereas, the AmIII vibration downshifts by ~4 cm^{-1}. The magnitude of the AmII frequency downshift between the dry, solid and the collapsed 45 °C aqueous PNIPAM nanogel

is similar to the temperature induced frequency shift observed for the AmII vibration between 4° and 45 °C ($\Delta\nu = 6\ cm^{-1}$), indicating weakening of NH-water hydrogen bonding. The impact of particle dehydration on the AmI frequency is relatively small as compared to the large upshift observed in the PNIPAM nanogel in water between 4° and 45 °C. Spectral modeling of the AmI region with three Gaussians indicates that the 7 cm^{-1} upshift in the AmI region derives from a ~49% increase in the A and B hydrogen bonded amides (1654 cm^{-1} peak) as compared to the collapsed 45 ºC aqueous state (Fig 7).

The $C_\alpha H_b$ band intensity is slightly greater in the solid state as compared to the collapsed aqueous phase (Fig 7). The $C_\alpha H_b$ band intensity is sensitive to changes in coupling between the $C_\alpha H$ and N-H_b motions. The strength of coupling between the two motions in inversely correlated with the distance between the two hydrogens.[88] Thus, the increased $C_\alpha H_b$ band intensity indicates that the conformation of the amide bonds in the solid, dry state differs somewhat from their aqueous counterparts in that its ensemble structure favors a more extended conformations. There are also changes in the AmIII band shape which also indicate some Ψ-angle conformation alterations for some of the pendent amides.

The presence in dry PNIPAM of the 1654 cm^{-1} AmI band which we observe for A and B hydrogen bonded peptide bonds in water, probably derives from inter-chain hydrogen bonding between pendent amides. The formation of hydrogen bonded inter-chain aggregates is likely responsible for conformation changes at the amide bond as indicated by increased $C_\alpha H_b$ band intensity in the dry solid.

A Model of PNIPAM Collapse

In PNIPAM, our results indicate that at low temperatures the amide bonds are predominantly water-exposed. Likely at low temperatures the amides of PNIPAM are in an extended, trans amide conformation, as indicated by a strong $C_\alpha H_b$ band (Fig 4), that allows for favorable interactions between the amide and a surrounding hydration shell.[89] In the extended state the exposed amide bonds provide three hydrogen bonding sites where three water molecules localize and serve as nucleating sites for formation of large water clusters i.e. the hydration shells. The formation of these water cluster is highly cooperative, e.g. cooperative effects in a water pentamer cluster result in hydrogen bonds energies that are almost twice as large as the linear hydrogen bonded dimer.[90] Presumably, by providing a nucleation site the amide bond lowers the free energy barrier to formation of large water clusters. The free energy gained via formation of large water-clusters stabilizes the well-hydrated extended PNIPAM conformation.

At elevated temperatures, increased thermal agitation disrupts the extensive hydrogen bonding network that stabilizes these large water clusters. The loss of favorable interactions destabilizes the exposed PNIPAM conformation with its significantly exposed hydrophobic surface area. PNIPAM then collapses to a compact conformation that reduces its hydrophobic solvent accessible surface area. Such a compact state may be formed by pushing the *i*, *i*+3 isopropyl groups closer together to form local hydrophobic pockets where the C=O groups are located inside the hydrophobic core (Fig 8) which results in a large upshift of the AmI band. Nearer-neighbor interactions are sterically forbidden.

The formation of a collapsed hydrophobic cluster or a nano-pocket reduces PNIPAM's exposed hydrophobic surface area. The loss of well-ordered water molecules from the hydrophobic group's solvation shell into the bulk increases the system entropy, thus stabilizing the compact PNIPAM conformation. Previously, Okada and Tanaka's numerical simulations of PNIPAM in water indicate the temperature of LCST depends upon the hydration cooperativity.[91] Daggett and co-workers[92] working with elastin-like peptides found that the hydrophobic collapse of elastin-like peptides is driven by changes in water's orientation entropy.

As shown in Fig 9, we observe similar temperature-induced spectral changes for single PNIPAM polymer chains (m.w. ~25, 000) as observed for cross-linked PNIPAM nanoparticles. Utilizing the same band decomposition routine used for PNIPAM nanogels (Fig 5) we find that a temperature increase form 24 °C to 42 °C results in an A and B hydrogen bonded population increase from ~33% to 47%, while the fully hydrated population shows an equivalent decrease. This result indicates that the VPT evident for PNIPAM nanoparticles also occurs in single PNIPAM polymer chains.

Kinetics of PNIPAM's hydrophobic collapse

We examined the dynamics of the VPT to see if the dynamics would give insight into the VPT reaction coordinate. As shown in Fig 10A, a 15 °C T-jump results in prompt changes in the PNIPAM amide UVRR spectra which occur at the shortest delay times resolved. As in the equilibrium spectra the spectral changes are most prominent for the AmI band. The difference spectra at longer times resemble the equilibrium difference spectrum (Fig 10A). The kinetic changes in the AmI region can be accurately modeled as a single exponential process which yields a time constant of 360 ± 85 ns (Fig 10B).

The PNIPAM amide dehydration appears complete within 1 Xs; we do not observe any significant change in the AmI region at longer time scales (Fig 10B insert). The prompt spectral changes in the AmII and AmIII regions are very similar to features observed by Lednev *et al*[62] in T-jump Raman measurements of an α-helical polyala peptide. They demonstrated that these changes derived from the temperature-induced frequency shifts independent of peptide structural changes.[62]

Our success in modeling the transient spectral changes as a single exponential indicates that at least kinetically the PNIPAM collapse occurs as a two-state process with no significant intermediates observed. Previous steady-state light scattering studies of single PNIPAM chains indicate the polymer collapse involves at-least two-intermediate states as suggested by small but significant temperature-dependent changes in $<R_g/R_h>$.[93] Our steady-state (Fig 6) and kinetic (Fig 10) results indicate that these intermediates do not significantly impact PNIPAM hydration during the polymer collapse.

Our results are consistent with previous kinetic studies of Wang *et al*[1] and Reese *et al*[3] that indicate a single exponential collapse of free PNIPAM particles with relaxation times of ~390 ns and ~120 ns, respectively. The observed time for the PNIPAM's hydrophobic collapse is similar to the folding time observed for small α-helical peptides[62] and some designed ultra-fast folding mini-proteins,[86,94,95] where folding is regarded as being essentially limited by solvent friction.[94,96–103] The rate of collapse in PNIPAM may also be limited by polymer and water diffusion.

Polymer collapse is likely limited by the rate at which distant part of the polymer can form contacts.[104–107] The rate of intra-chain contact formation or the rate of loop formation has been extensively studied in the context of protein folding.[104–107] These studies indicate that the rate of loop formation is limited by solvent viscosity and chain stiffness. For short peptide chains (<10 mers) in water the rate of loop formation appears to be ~10^7 s^{-1}.[105,107] The rate of loop formation decreases with increasing chain length but due to chain stiffness which limits the conformation space available to the polymer chain, the rate of loop formation levels off at ~10^5 s^{-1} for n> 20.[107]

Assuming amide dehydration in PNIPAM is limited by the rate of polymer collapse, the observed collapse rate in PNIPAM (10^6 s^{-1}) suggests an average persistence length in PNIPAM of n~10.[105,107] At lengths shorter than the persistence length the polymer acts as an elastic rod, whereas, at lengths longer than the persistence length the polymer backbone conformation

forms a random coil. The estimated persistence length is roughly three times longer than the smallest possible PNIPAM length required to form a local hydrophobic pocket. This suggests that probably the adjacent hydrophobic pockets coalesce via hydrophobic interactions to stabilize the collapsed particle.

PNIPAM chains as small as a 10-mer is thus expected to show a temperature induced hydrophobic collapse. It should be noted that a 10-mer is also the minimum length required for a polypeptide to fold into a stable α-helix conformation

Conclusions

PNIPAM has long been utilized as a model system for understanding temperature-induced polymer hydrophobic collapse. Here we utilize DLS, H-NMR, and steady-state UVRR measurements to determine that in the collapsed state the amide bonds of PNIPAM do not engage in inter-amide hydrogen bonding. Our measurements clearly indicate that above T_t the amide bonds of PNIPAM are predominantly hydrogen bonded on average to two water molecules each, with one water-peptide hydrogen bond at the C=O and N-H site each. In contrast at low temperatures the C=O is hydrogen bonded to two water molecules.

Based on our spectroscopic data we propose that at low temperatures the PNIPAM-water interactions stabilize an extended water-exposed conformation. At elevated temperatures, thermal agitation disrupts the solvation shell around *N*-isopropylacrylamide (NIPAM). The loss of favorable NIPAM-water solvation shell interactions forces the PNIPAM chain to adopt a compact conformation, forming local hydrophobic pockets that significantly reduce the solvent exposure of its pendent NIPAM amide groups. The resulting decrease in hydrophobic solvation increases the system entropy which stabilizes the compact/dehydrated state of PNIPAM.

Steric constraints prevent hydrophobic contacts between nearest neighbors. The (*i*, *i*+3) is the nearest neighbor pair that can form hydrophobic contacts free of steric clashes (Fig 8). The formation of local hydrophobic clusters results in a loss on average of one C=O-water hydrogen bond, which results in a 28 cm^{-1} upshift in the average AmI frequency. This provides a convenient marker for examining the temporal evolution of the PNIPAM collapse.

Our time-resolved UVRR measurements indicate that the changes in C=O-water hydrogen bonding can be modeled as a mono-exponential collapse with a time constant of 360 (± 80) ns. Changes in the AmII region are complete within 60 ns, indicating the AmII frequency shifts derive from temperature induced weakening of NH-water hydrogen bonds. Similar temperature induced changes in the amide band frequencies were observed by Lednev et al[62] in their T-jump study of a mainly α-helical peptide. Thus, the NH hydrogen bonding does not appear to significantly change.

Assuming the PNIPAM collapse is diffusion limited, the rate of collapse (10^6 s^{-1}) suggests a persistence length of n~10. The estimated persistence length is ~3-times longer than the shortest polymer length that is sterically allowed to form a hydrophobic cluster. This suggests that the hydrophobic collapse is a cooperative process where probably adjacent hydrophobic pockets coalesce via hydrophobic interactions to stabilize the collapsed particle.

The hydrophobic collapse of PNIPAM is driven by changes in polymer-water interactions. In the extended state the exposed amide bonds provide three hydrogen bonding sites where water molecules localize and serve as nucleating sites for formation of large water clusters i.e. a hydration shell. The formation of these water clusters is highly cooperative, e.g. cooperative effects in a water pentamer cluster result in hydrogen bonds energies that are almost twice as large as the linear hydrogen bonded dimer.[90] Presumably, by providing a nucleation site the

amide bond lowers the free energy barrier to formation of large water clusters. The free energy gained via formation of large water-clusters stabilizes the well-hydrated extended PNIPAM conformation.

At elevated temperatures, increased thermal agitation disrupts the extensive hydrogen bonding network that stabilizes the large water cluster. The loss of favorable interactions destabilizes the exposed PNIPAM conformation with its significantly exposed hydrophobic surface area. PNIPAM then collapses to a compact conformation that reduces it hydrophobic solvent accessible surface area. The loss of well-ordered water molecules from the hydrophobic group's solvation shell into the bulk increases the system entropy, thus stabilizing the compact PNIPAM conformation. Our results here suggest that PNIPAM hydrophobic collapse is driven by temperature-induced changes in water hydrogen bonding.

Acknowledgements

The authors would like to thank Prof. David Earl and Prof. Ken Jordon and Dr. Adam Hixon for helpful discussions, Dr. Damodaran Krishnan for help with H-NMR measurements and NIH grant RO1 EB002053 for financial support.

References

1. Wang J, Gan D, Lyon LA, El-Sayed MA. Journal of the American Chemical Society 2001;123:11284. [PubMed: 11697971]
2. Wang X, Wu C. Macromolecules 1999;32:4299.
3. Reese CE, Mikhonin AV, Kamenjicki M, Tikhonov A, Asher SA. Journal of the American Chemical Society 2004;126:1493. [PubMed: 14759207]
4. Tiktopulo EI, Uversky VN, Lushchik VB, Klenin SI, Bychkova VE, Ptitsyn OB. Macromolecules 1995;28:7519.
5. Katsumoto Y, Tanaka T, Ozaki Y. Macromolecular Symposia 2004;205:209.
6. Katsumoto Y, Tanaka T, Sato H, Ozaki Y. Journal of Physical Chemistry A 2002;106:3429.
7. Saunders BR, Crowther HM, Morris GE, Mears SJ, Cosgrove T, Vincent B. Colloids and Surfaces, A: Physicochemical and Engineering Aspects 1999;149:57.
8. Saunders BR, Vincent B. Advances in Colloid and Interface Science 1999;80:1.
9. Yi Y, Oh KS, Bae YH. Polymer 1997;38:3471.
10. Cimen EK, Rzaev ZMO, Piskin E. Journal of Applied Polymer Science 2005;95:573.
11. Crowther HM, Saunders BR, Mears SJ, Cosgrove T, Vincent B, King SM, Yu GE. Colloids and Surfaces, A: Physicochemical and Engineering Aspects 1999;152:327.
12. Ding Z, Chen G, Hoffman AS. Journal of Biomedical Materials Research 1998;39:498. [PubMed: 9468062]
13. Harmon ME, Frank CW. ACS Symposium Series 2003;833:2.
14. Inoue T, Chen G, Nakamae K, Hoffman AS. Polymer Gels and Networks 1998;5:561.
15. Mendez S, Curro JG, McCoy JD, Lopez GP. Macromolecules 2005;38:174.
16. Zeng F, Tong Z, Feng H. Polymer 1997;38:5539.
17. Zhao Y, Cao Y, Yang Y, Wu C. Macromolecules 2003;36:855.
18. Mao H, Li C, Zhang Y, Furyk S, Cremer PS, Bergbreiter DE. Macromolecules 2004;37:1031.
19. Gan D, Lyon LA. Journal of the American Chemical Society 2001;123:7511. [PubMed: 11480971]
20. Hoare T, Pelton R. Langmuir 2004;20:2123. [PubMed: 15835661]
21. Dufresnea MH, Garreca DL, Santa V, Lerouxa JC, Range M. International Journal of Pharmaceutics 2004;277:81. [PubMed: 15158971]
22. Bergbreiter DE, Case BL, Liu YS, Caraway JW. Macromolecules 1998;31:6053.
23. Jiang X, Xiong D, Zheng P, Zhang W, Shi L. Journal of Polymer Science Part A: Polymer Chemistry 2007;45:2812.
24. Zhang Y, Guan Y, Zhou S. Biomacromolecules 2006;7:3196. [PubMed: 17096551]

25. Iwai K, Matsumura Y, Uchiyama S, de Silva AP. Journal of Materials Chemistry 2005;15:2796.
26. Barker IC, Cowie JMG, Huckerby TN, Shaw DA, Soutar I, Swanson L. Macromolecules 2003;20:7765.
27. Annaka M, Motokawa K, Sasaki S, Nakahira T, Kawasaki H, Maeda H, Amo Y, Tominaga Y. Journal of Chemical Physics 2000;113:5980.
28. Annaka M, Amo Y, Sasaki S, Tominaga Y, Motokawa K, Nakahira T. Physical Review E: Statistical, Nonlinear, and Soft Matter Physics 2002;65:031805/1.
29. Annaka M, Tanaka C, Nakahira T, Sugiyama M, Aoyagi T, Okano T. Macromolecules 2002;35:8173.
30. Suzuki Y, Suzuki N, Takasu Y, Nishio I. Journal of Chemical Physics 1997;107:5890.
31. Terada T, Inaba T, Kitano H, Maeda Y, Tsukida N. Macromolecular Chemistry and Physics 1994;195:3261.
32. Appel R, Zerda TW, Wang C, Hu Z. Polymer 2000;42:1561.
33. Appel R, Xu W, Zerda TW, Hu Z. Macromolecules 1998;31:5071. [PubMed: 9680447]
34. Meersman F, Wang J, Wu YKH. Macromolecules 2005;38:8923.
35. Ono O, Shikata T. J Am Chem Soc 2006;128:10030. [PubMed: 16881629]
36. Ono Y, Shikata T. J Phys Chem B 2007;111:1511. [PubMed: 17266365]
37. Ahmed Z, Scaffidi J, Asher SA. Biopolymers. 2008in press
38. Urry DW, Parker TM. Journal of Muscle Research and Cell Motility 2002;23:543. [PubMed: 12785104]
39. Tamburro AM, Bochicchio B, Pepe A. Biochemistry 2003;42:13347. [PubMed: 14609345]
40. Rodriguez-Cabello JC, Alonso M, Diez MI, Caballero MI, Herguedas MM. Macromolecular Chemistry and Physics 1999;200:1831.
41. Alonso M, Reboto V, Guiscardo L, San Martin A, Rodriguez-Cabello JC. Macromolecules 2000;33:9480.
42. Tsai C-J, Maizel JV Jr, Nussinov R. Critical Reviews in Biochemistry and Molecular Biology 2002;37:55. [PubMed: 12027264]
43. Tauc, P.; Fusi, P.; Tortora, P.; Lange, R.; Brochon, JC. Advances in High Pressure Bioscience and Biotechnology; Proceedings of the International Conference; Heidelberg. Aug 30-Sept 3 1998–1999; p. 191
44. Tang Xiaolin C, Pikal Michael J. Pharmaceutical research 2005;22:1167. [PubMed: 16028018]
45. Tamura A. Netsu Sokutei 1995;22:186.
46. Graziano G, Catanzano F, Riccio A, Barone G. Journal of Biochemistry (Tokyo) 1997;122:395.
47. Goto Y. Baiosaiensu to Indasutori 2002;60:235.
48. Andersen NH, Cort JR, Liu Z, Sjoberg SJ, Tong H. Journal of the American Chemical Society 1996;118:10309.
49. Privalov PL, Griko YV, Venyaminov SY, Kutyshenko VP. Journal of Molecular Biology 1986;190:487. [PubMed: 3783710]
50. Privalov PL. Critical Reviews in Biochemistry and Molecular Biology 1990;25:281. [PubMed: 2225910]
51. Weissman JM, Sunkara HB, Tse AS, Asher SA. Science 1996;274:959. [PubMed: 8875932]
52. Tanaka T, Fillmore DJ. Journal of Chemical Physics 1979;70:1214.
53. Tanaka T, Hocker LO, Benedek GB. Journal of Chemcial Physics 1973;59:5151.
54. Maeda Y, Higuchi T, Ikeda I. Langmuir 2000;16:7503.
55. Maeda Y, Nakamura T, Ikeda I. Macromolecules 2001;34:1391.
56. Maeda Y, Nakamura T, Ikeda I. Macromolecules 2001;34:8246.
57. Maeda Y, Taniguchi N, Ikeda I. Macromolecular Rapid Communications 2001;22:1390.
58. Maeda Y, Yamamoto H, Ikeda I. Macromolecules 2003;36:5055.
59. Maeda Y, Yamamoto H, Ikeda I. Colloid and Polymer Science 2004;282:1268.
60. Lin SY, Chen KS, Run-Chu L. Polymer 1999;40:2619.
61. Bykov SB, Lednev IK, Ianoul A, Mikhonin AV, Asher SA. Appl Spectrosc 2005;59:1541. [PubMed: 16390595]

62. Lednev IK, Karnoup AS, Sparrow MC, Asher SA. J Am Chem Soc 1999;121:8074.
63. Williams S, Causgrove TP, Gilmanshin R, Fang KS, Callender RH, Woodruff WH, Dyer RB. Biochemistry 1996;35:691. [PubMed: 8547249]
64. Torii H, Tasumi M. Journal of Raman Spectroscopy 1998;29:81.
65. Torii H, Tasumi M. International Journal of Quantum Chemistry 1998;70:241.
66. Chen XG, Schweitzer-Stenner R, Asher SA, Mirkin NG, Krimm S. J Phys Chem 1995;99:3074.
67. Mikhonin AV, Ahmed Z, Ianoul A, Asher SA. Journal of Physical Chemistry B 2004;108:19020.
68. Chi Z, Chen XG, Holtz JSW, Asher SA. Biochemistry 1998;37:2854. [PubMed: 9485436]
69. Asher SA, Ianoul A, Mix G, Boyden MN, Karnoup A, Diem M, Schweitzer-Stenner R. J Am Chem Soc 2001;123:11775. [PubMed: 11716734]
70. Wang Y, Purrello R, Jordan T, Spiro TG. Journal of the American Chemical Society 1991;113:6359.
71. Wang Y, Purrello R, Spiro TG. Journal of the American Chemical Society 1989;111:8274.
72. Pan YV, Wesley RA, Luginbuhl R, Denton DD, Ratner BD. Biomacromolecules 2001;2:32. [PubMed: 11749152]
73. Mikhonin AV, Bykov SV, Myshakina NS, Asher SA. J Phys Chem B 2006;110:5509.
74. Myshakina NS, Ahmed Z, Asher SA. J Phys Chem B 2008;112:11873. [PubMed: 18754632]
75. Torii H, Tatsumi T, Tasumi M. J Raman Spectrosc 1998;29:537.
76. Manas ES, Getahun Z, Wright WW, DeGrado WF, Vanderkooi JM. J Am Chem Soc 2000;122:9883.
77. Torii H, Tatsumi T, Kanazawa T, Tasumi M. Journal of Physical Chemistry B 1998;102:309.
78. Torii H, Tatsumi T, Tasumi M. Mikrochimica Acta, Supplement 1997;14:531.
79. Dioumaev AK, Brainman MS. J Am Chem Soc 1995;117:10572.
80. Simonson T, Brooks CL III. J Am Chem Soc 1996;118:8452.
81. Simonson T, Perahia D. Proc Nat Acad Sci USA 1995;92:1082. [PubMed: 7862638]
82. Dwyer JJ, Gittis AG, Karp DA, Lattman EE, Spencer DS, Stites WE, Garcia-Moreno E. B Biophys J 2000;79:1610.
83. Triggs NE, Valentini JJ. J Phys Chem 1992;96:6922.
84. Mayne LC, Hudson B. J Phys Chem 1991;95:2962.
85. Ahmed Z, Asher SA. Biochemistry 2006;45:9068. [PubMed: 16866352]
86. Ahmed Z, Illir AB, Mikhonin AV, Asher SA. J Am Chem soc 2005;127:10943. [PubMed: 16076200]
87. Wang Y, Purrello R, Georgiou S, Spiro TG. Journal of the American Chemical Society 1991;113:6368.
88. Asher SA, Ianoul A, Mix G, Boyden MN, Karnoup A, Diem M, Schweitzer-Stenner R. Journal of the American Chemical Society 2001;123:11775. [PubMed: 11716734]
89. Mezei M, Fleming PJ, Srinivasan R, Rose GD. Proteins: Structure, Function, and Bioinformatics 2004;55:502.
90. Ludwig R. Angew Chem Int Ed 2001;40:1808.
91. Okada Y, Tanaka F, Kujawa P, Winnik FM. Journal of Chemcial Physics 2006;125:244902.
92. Li B, Alonso DOV, Bennion BJ, Daggett V. Journal of the American Chemical Society 2001;123:11991. [PubMed: 11724607]
93. Wu C, Wang X. Physical review letters 1998;80:4092.
94. Qiu L, Pabit SA, Roitberg AE, Hagen SJ. Journal of the American Chemical Society 2002;124:12952. [PubMed: 12405814]
95. Dyer RB, Gai F, Woodruff WH. Acc Chem Res 1998;31:709.
96. Bieri O, Wirz J, Hellrung B, Schutkowski M, Drewello M, Kiefhaber T. Proceedings of the National Academy of Sciences of the United States of America 1999;96:9597. [PubMed: 10449738]
97. Hagen SJ, Qiu L, Pabit SA. Journal of Physics: Condensed Matter 2005;17:S1503.
98. Kubelka J, Buscaglia M, Hofrichter J, Eaton WA. NATO Science Series, Series I: Life and Behavioural Sciences 2005;364:1.
99. Kubelka J, Hofrichter J, Eaton WA. Current Opinion in Structural Biology 2004;14:76. [PubMed: 15102453]

100. McCammon JA. Proceedings of the National Academy of Sciences of the United States of America 1996;93:11426. [PubMed: 8876151]
101. Nguyen H, Jaeger M, Kelly JW, Gruebele M. Journal of Physical Chemistry B 2005;109:15182.
102. Pabit SA, Roder H, Hagen SJ. Biochemistry 2004;43:12532. [PubMed: 15449942]
103. Qiu L, Hagen SJ. Journal of the American Chemical Society 2004;126:3398. [PubMed: 15025447]
104. Fierz B, Kiefhaber T. J Am Chem Soc 2007;129:672. [PubMed: 17227031]
105. Krieger F, Moeglich A, Kiefhaber T. Journal of the American Chemical Society 2005;127:3346. [PubMed: 15755151]
106. Lapidus LJ, Steinbach PJ, Eaton WA, Szabo A, Hofrichter J. J Phys Chem B 2002;106:11628.
107. Lee JC, Lai BT, Kozak JJ, Gray HB, Winkler JR. J Phys Chem B 2007;111:2107. [PubMed: 17279794]

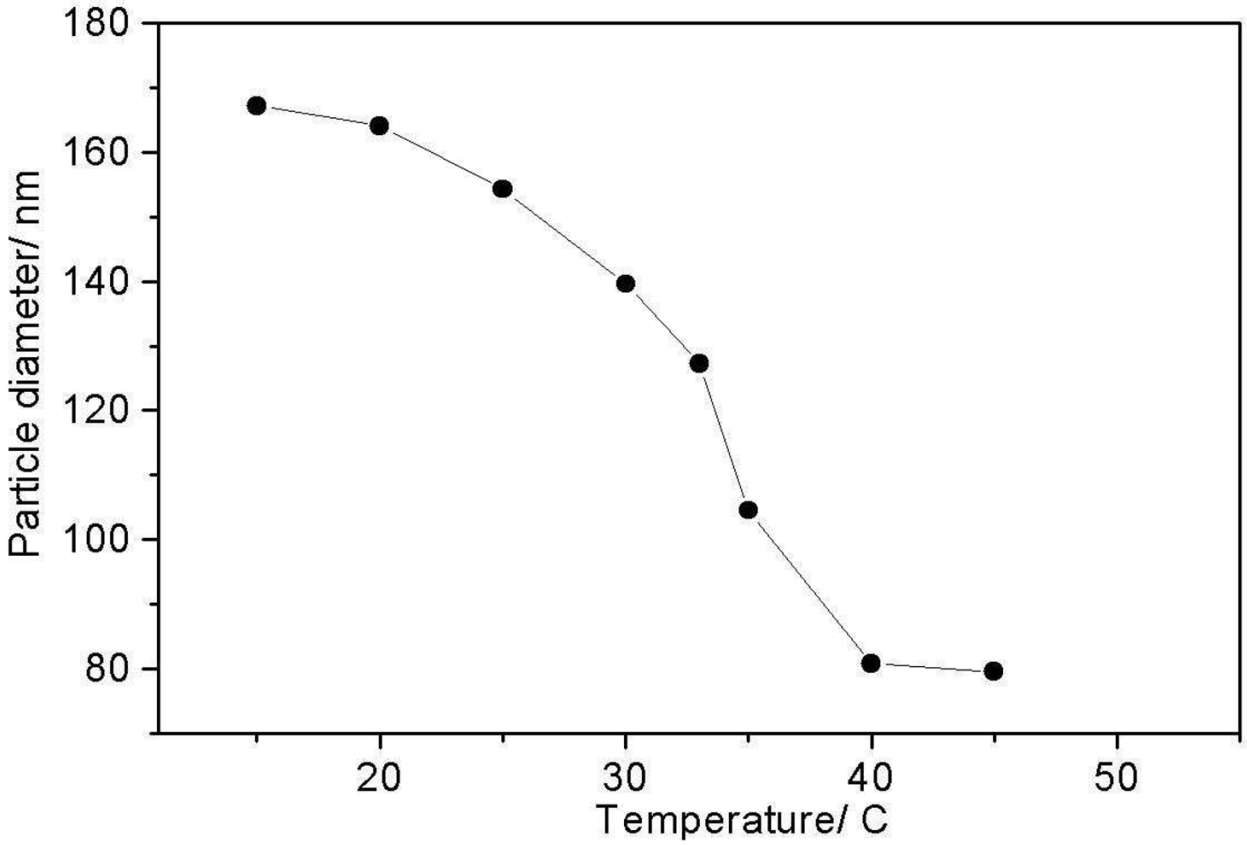

Figure 1.
Temperature dependent DLS measurements show that PNIPAM particles collapse between 20 °C and 40 °C with a transition temperature of ~33 °C

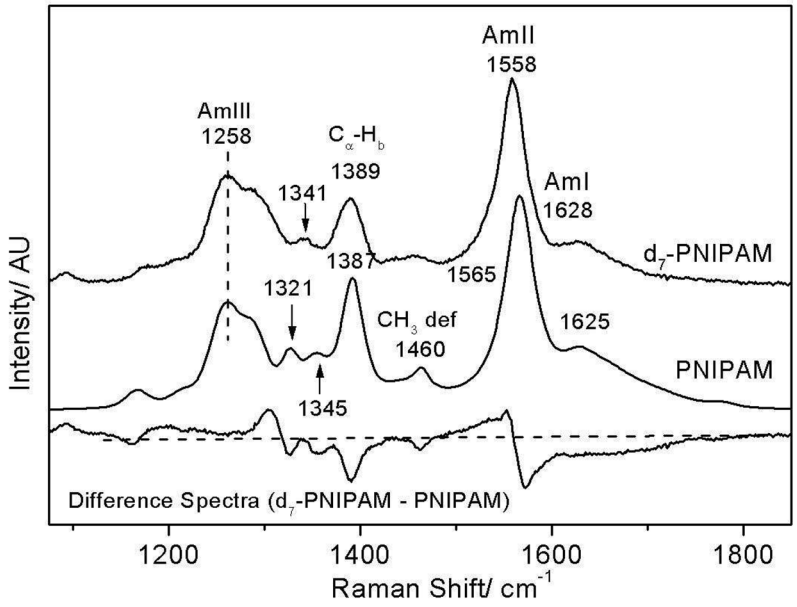

Figure 2.

204 nm excited UV Raman spectra of PNIPAM and d_7-PNIPAM at 5 °C. Both spectra were normalized to the peak intensity of their AmIII bands. The difference spectrum was obtained by subtracting the PNIPAM spectra from that of d_7-PNIPAM.

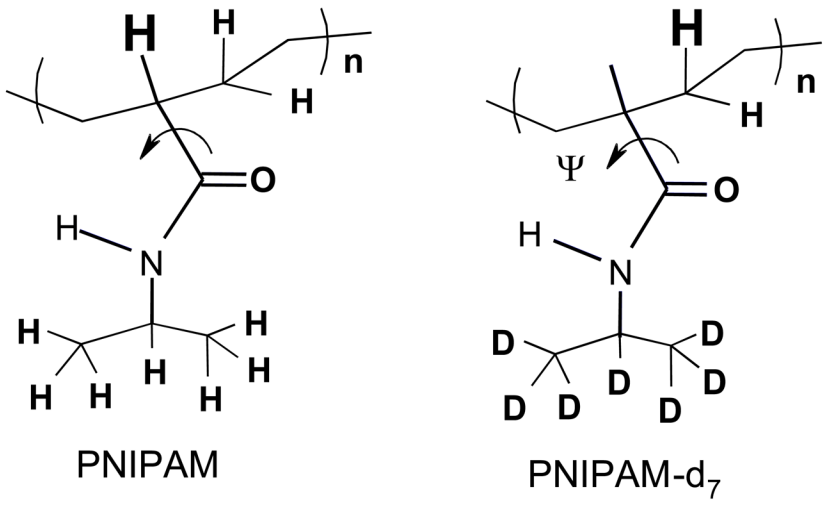

Figure 3.

The structure of PNIPAM and its deuterated isotopomers, d_7-PNIPAM. The C_α-hydrogen that gives rise to the resonance enhanced $C_\alpha H_b$ band at ~1387 cm^{-1} is highlighted. The curved arrow highlights the Ψ dihedral angle rotation around the C_α-C(O) bond. The AmIII band frequency is sensitive to the Ramachandran Ψ angle rotation around the C_α-C(O) bond.

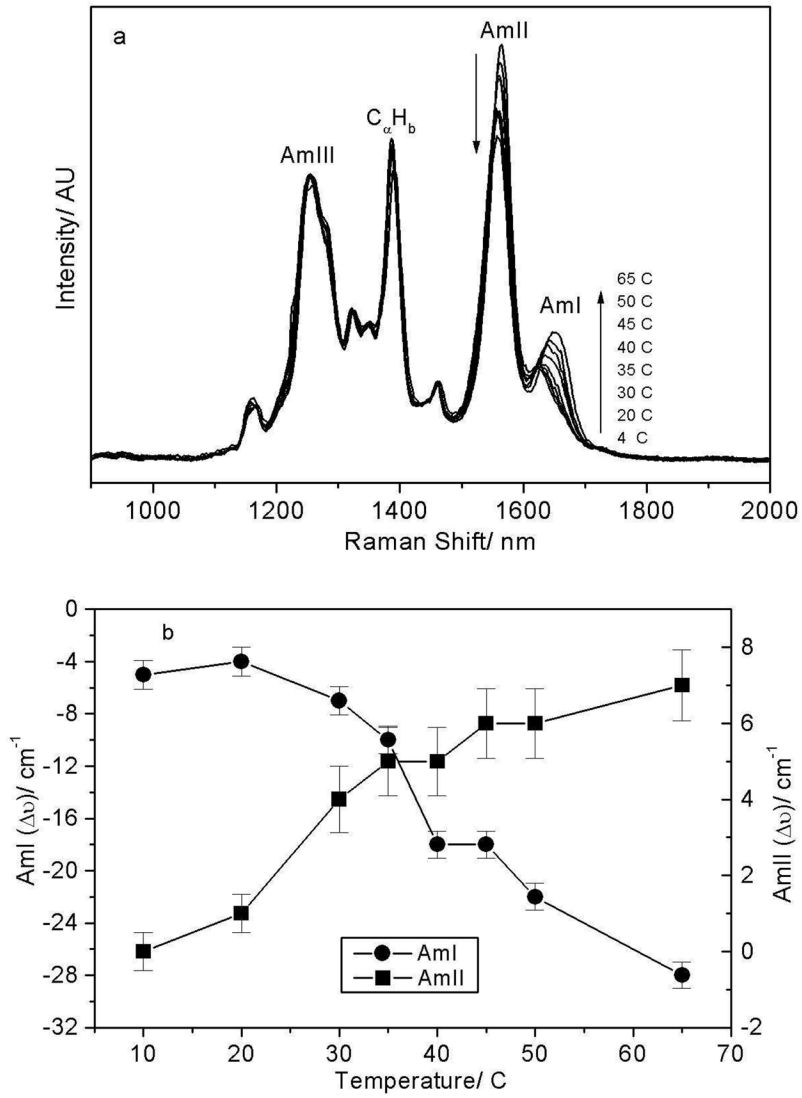

Figure 4.

Temperature dependence of the 204 nm excited UVRR spectra of PNIPAM. The AmI band intensity increases and upshifts with temperature, while the AmII band intensity decreases and downshifts with temperature.

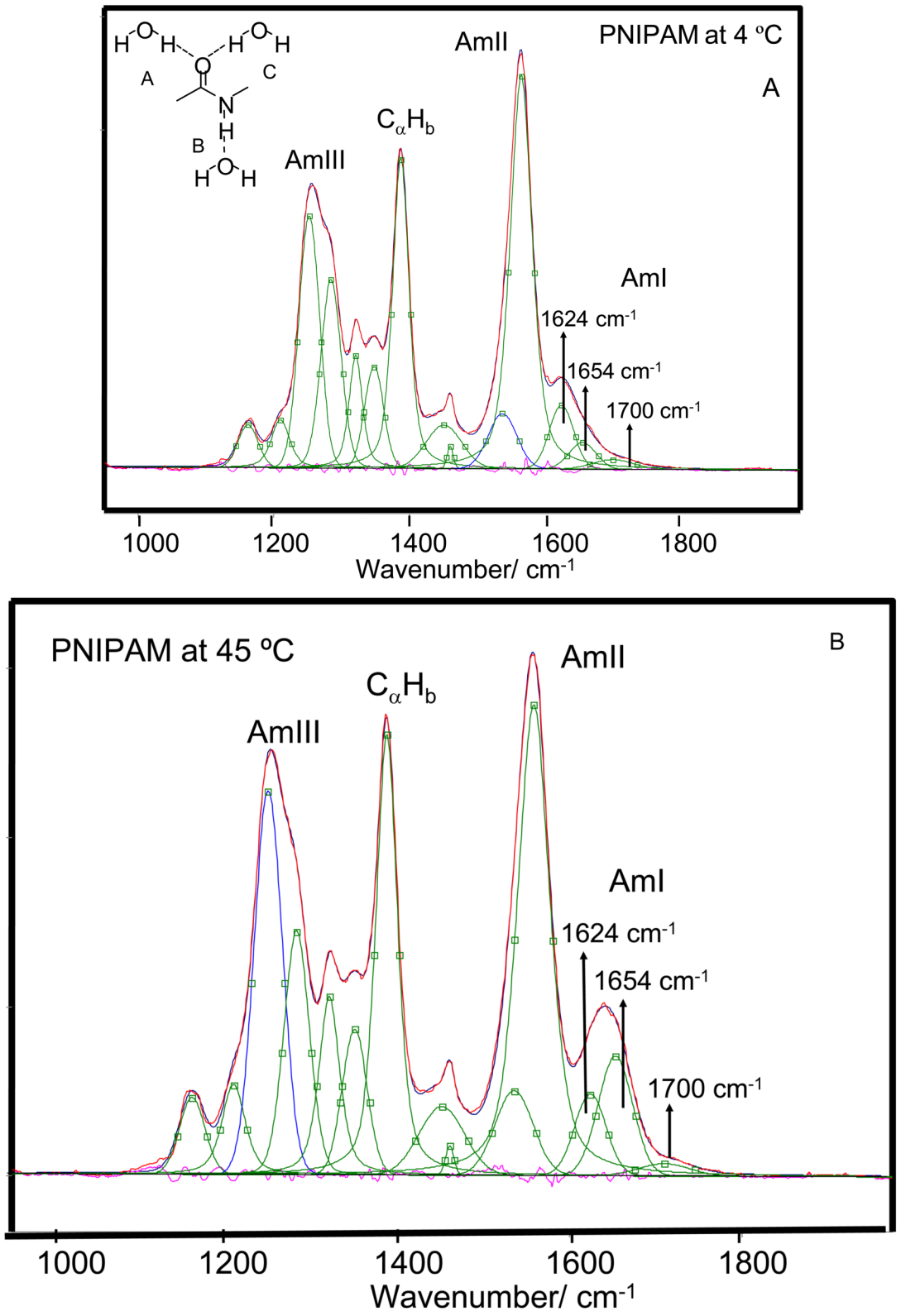

Figure 5.

204-nm excited UVRR spectra of PNIPAM at (A) 4 °C and (B) 45 °C the spectra were decomposed into a minimum sum of mixed Lorentzian and Gaussian bands. The AmI region was fit to Gaussian bands. The measured and modeled spectra overlap almost completely. The different amide-hydrogen bonding sites are shown in the Fig 5A insert.

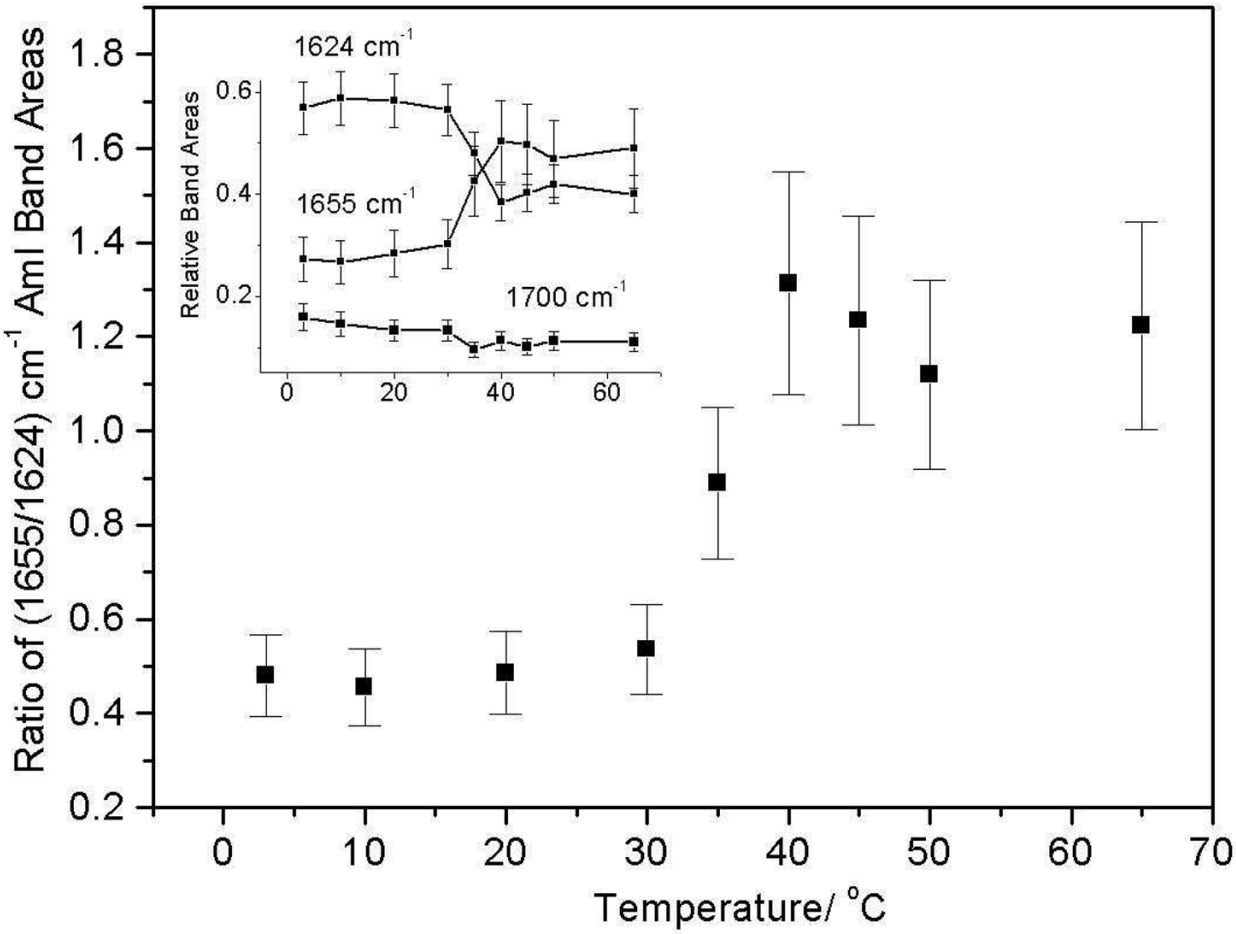

Figure 6.
The intensity ratio of the 1655 cm^{-1}/1624 cm^{-1} AmI bands shows an abrupt increase between 30 °C and 40 °C.

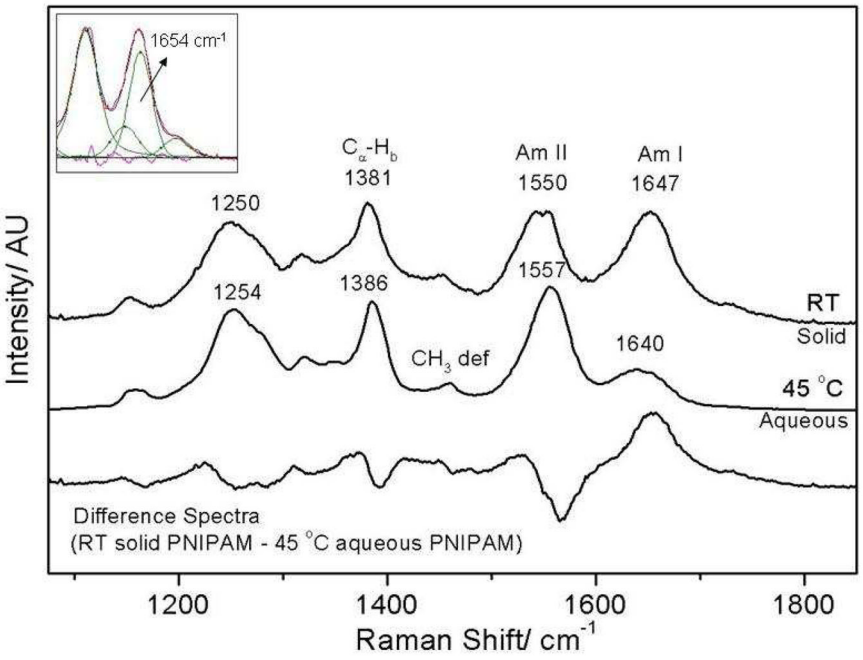

Figure 7.

PNIPAM spectra in water (45 °C) and in the solid dehydrated state normalized to the peak intensity of the AmIII bands show significant differences in the amide band frequencies. In particular, the AmI vibration upshifts while, the AmII vibration downshifts by 7 cm^{-1} upon PNIPAM dehydration. The insert shows the results of spectral decomposition in the AmI and AmII region of the dry, solid PNIPAM which show increased band intensity for the 1654 cm^{-1} AmI region.

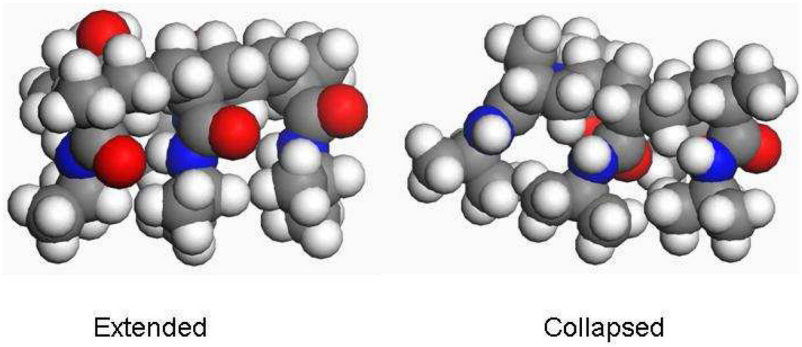

Figure 8.
A cartoon of collapsed and extended conformation of PNIPAM (top-view) as drawn in Material Studio software. Note that the carbonyl groups are fully exposed in the extended conformation but are located inside the hydrophobic pocket in the collapsed state. The carbonyl oxygens are colored red while, the nitrogens are blue.

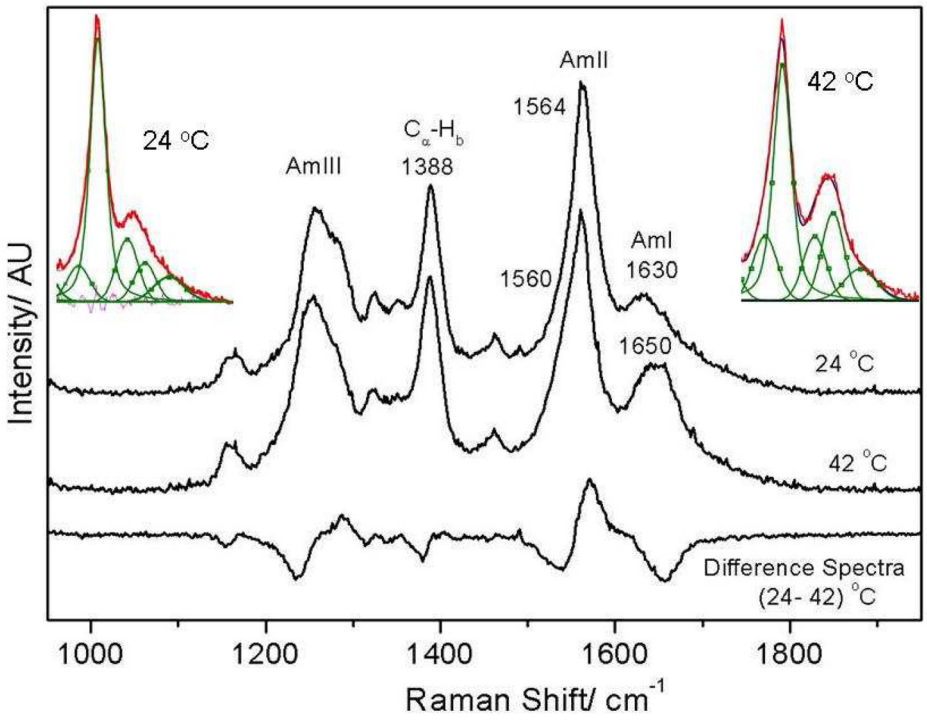

Figure 9.

Single chain PNIPAM shows a ~20 cm^{-1} upshift in the AmI vibrational frequency upon PNIPAM collapse. Spectral decomposition of the AmI and AmII regions at 24 and 42 ºC are shown in inserts.

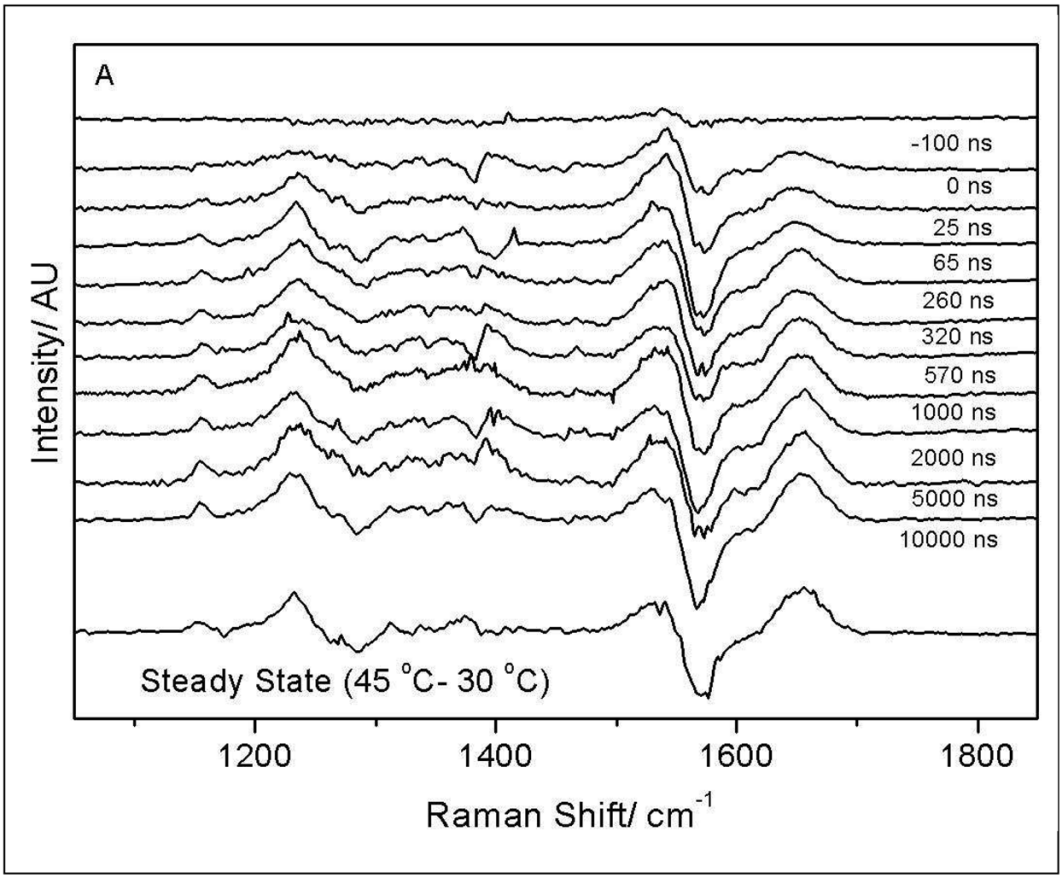

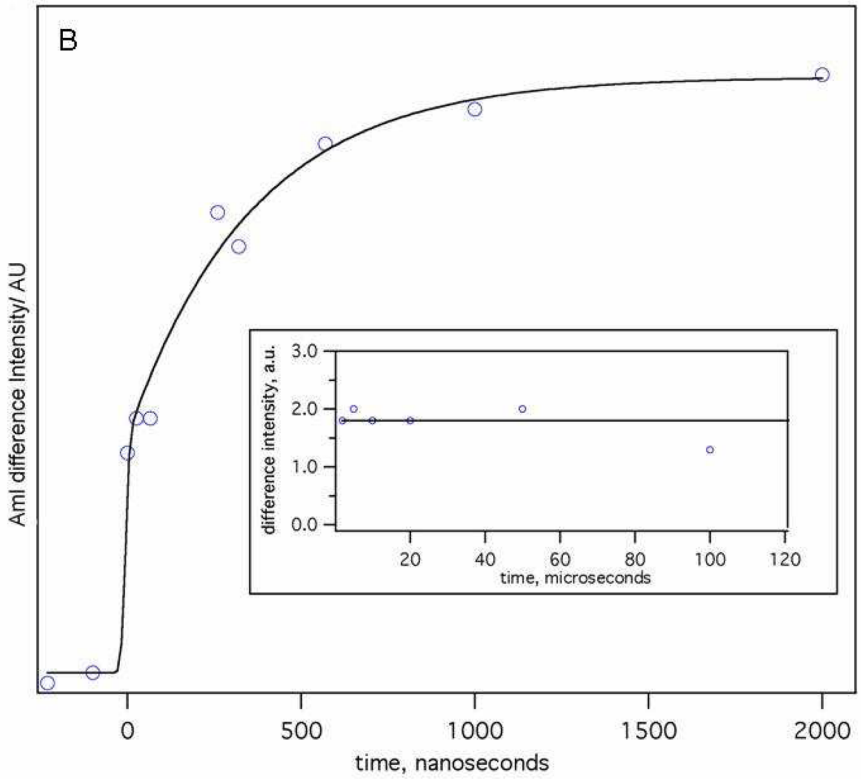

Figure 10.

A) Time resolved 204-nm UVRR (hot – 30 °C) difference spectra at different delay times. The AmI band shows the largest spectral shift. B) The peak to peak AmI band intensity in the (hot – 30 °C) transient difference spectra at different delay time is used to model the kinetics of PNIPAM's hydrophobic collapse. All changes in the AmI region are complete within 1 μs; we do not observe any significant changes in the AmI region at longer timescales (insert). The amide band intensity in the difference spectra shows a small decrease at 100 μs which indicates sample volume cooling due to thermal diffusion and equilibration.